

Energetics of a two-phase model of lithospheric damage, shear localization and plate-boundary formation

David Bercovici¹ and Yanick Ricard²

¹Department of Geology and Geophysics, Yale University, PO Box 208109, New Haven, CT 06520-8109, USA. E-mail: david.bercovici@yale.edu

²Laboratoire des Sciences de la Terre, Ecole Normale Supérieure de Lyon, 46 allée d'Italie, F-69364 Lyon, Cedex 07, France. E-mail: ricard@ens-lyon.fr

Accepted 2002 August 21. Received 2002 July 29; in original form 2002 January 22

SUMMARY

The two-phase theory for compaction and damage proposed by Bercovici *et al.* (2001a, *J. Geophys. Res.*, **106**, 8887–8906) employs a nonequilibrium relation between interfacial surface energy, pressure and viscous deformation, thereby providing a model for damage (void generation and microcracking) and a continuum description of weakening, failure and shear localization. Here we examine further variations of the model which consider (1) how interfacial surface energy, when averaged over the mixture, appears to be partitioned between phases; (2) how variability in deformational-work partitioning greatly facilitates localization; and (3) how damage and localization are manifested in heat output and bulk energy exchange. Microphysical considerations of molecular bonding and activation energy suggest that the apparent partitioning of surface energy between phases goes as the viscosity of the phases. When such partitioning is used in the two-phase theory, it captures the melt-compaction theory of McKenzie (1984, *J. Petrol.*, **25**, 713–765) exactly, as well as the void-damage theory proposed in a companion paper (Ricard & Bercovici, submitted). Calculations of 1-D shear localization with this variation of the theory still show at least three possible regimes of damage and localization: at low stress is weak localization with diffuse slowly evolving shear bands; at higher stress strong localization with narrow rapidly growing bands exists; and at yet higher shear stress it is possible for the system to undergo broadly distributed damage and no localization. However, the intensity of localization is strongly controlled by the variability of the deformational-work partitioning with dilation rate, represented by the parameter γ . For $\gamma \gg 1$, extreme localization is allowed, with sharp profiles in porosity (weak zones), nearly discontinuous separation velocities and effectively singular dilation rates. Finally, the bulk heat output is examined for the 1-D system to discern how much deformational work is effectively stored as surface energy. In the high-stress, distributed-damage cases, heat output is reduced as more interfacial surface energy is created. Yet, in either the weak or strong localizing cases, the system always releases surface energy, regardless of the presence of damage or not, and thus slightly more heat is in fact released than energy is input through external work. Moreover, increased levels of damage (represented by the maximum work-partitioning f^*) make the localizing system release surface energy faster as damage enhances phase separation and focusing of the porosity field, thus yielding more rapid loss of net interfacial surface area. However, when cases with different levels of damage are compared at similar stages of development (say, the peak porosity of the localization) it is apparent that increased damage causes smaller relative heat release and retards loss of net interfacial surface energy. The energetics and energy partitioning of this damage and shear-localization model are applied to estimating the energy costs of forming plate boundaries and generating plates from mantle convection.

Key words: geodynamics, lithospheric deformation, plate tectonics.

1 INTRODUCTION

Because of its high viscosity and creeping motion over geological timescales, the lithosphere–mantle system is considered highly

dissipative. Thus, models of mantle convection generally assume that convective work, or the release of gravitational potential energy, is completely dissipated as viscous or frictional heating. However, materials science has provided evidence since early in the 20th

century (if not earlier) that not all deformational work is dissipated as heat and that some such work is effectively stored as internal energy associated with defects, microcracks and dislocations in the material. In the 1920's and 1930's, G.I. Taylor performed experiments on torsional deformation of metals and found that a fraction of deformational work (termed 'cold work') was stored as internal energy that later, upon heating and annealing, was released as latent heat (Farren & Taylor 1925; Taylor & Quinney 1934). Few similar analyses have been performed in the last 20 yr, for example the experimental work of A. Chrysochoos on thermometric measurements of deformed materials (Chrysochoos & Martin 1989; Chrysochoos *et al.* 1989, 1996).

The partitioning of deformational work between dissipation and stored energy is now a common assumption in studies of dilatant plasticity, damage and shear localization in metals and industrial materials (e.g. ceramics) (Lemonds & Needleman 1986; Povirk *et al.* 1994; Mathur *et al.* 1996; Hansen & Schreyer 1992; Lemaitre 1992) as well as in fault dynamics (Lyakhovskiy *et al.* 1997) and continental collision zones (Regenauer-Lieb 1999). Partitioning of work between heat, stored energy and seismic radiation is also an important fundamental problem in the physics of earthquake and is referred to as seismic efficiency (Mora & Place 1998).

In a similar fashion, the viscous two-phase damage theory previously proposed by us (Bercovici *et al.* 2001a; Ricard *et al.* 2001; Bercovici *et al.* 2001b) to treat lithospheric strain localization and plate boundary formation, has as its core assumption that a fraction f of the deformational work is stored as energy on microcrack surfaces, which is represented as interfacial surface energy. Three aspects of energy partitioning and stored energy are thus further explored in this paper.

First, in the two-phase damage theory, the stored energy is manifest as surface energy on the interface between the two phases, which themselves represent the host material (rock) and void-filling material (fluid such as water). However, as with most two-phase or mixture theories, neither the location of phase elements (pores of void fluid and grains of host matrix) nor the interface between phases is delineated. With mathematical averaging, the phases and interface are treated as continuous entities, existing at all points in the domain but in various concentrations. The fluid is represented as existing at all points with a volumetric concentration of ϕ , otherwise known as the porosity; the host matrix exists with volumetric concentration $1 - \phi$; and the interface exists with areal concentration (i.e. interfacial surface area per unit volume) α (Drew & Segel 1971; Ni & Beckerman 1991; Bercovici *et al.* 2001a). The interfacial surface tension force imparted to each phase is likewise mathematically distributed over the domain and thereby treated as an effective body force acting internally through the mixture volume and on each phase. The surface energy is similarly distributed mathematically and thus assumed to be carried volumetrically like an internal energy by each phase. How the surface tension and energy are assumed to be effectively distributed between phases raises a separate partitioning assumption, i.e. how surface energy/tension is partitioned between phases. Bercovici *et al.* (2001a) assumed that surface energy is, in effect, equipartitioned between the phases. However, in this paper, we consider the microphysical relation between surface energy and material properties of phases such as molecular bond strength and viscosity. From these considerations we propose a possibly more realistic surface-energy partitioning assumption which also improves the self-consistency of the theory and allows for an exact correspondence with the two-phase melt-dynamics theory of McKenzie (1984) and Spiegelman (1993a,b,c).

With this variation of our two-phase damage theory, we re-examine some fundamental 1-D shear-localization cases and investigate the various aspects of deformational work partitioning. The work partitioning fraction f was shown by Bercovici *et al.* (2001b) to vary with at least dilation rate, the variability represented by the parameter γ . The influence of both the maximum allowable partitioning $f^* = \max(f)$ and dilation-rate dependence γ are examined for their influence on localization. As will be shown here, γ strongly controls the sharpness and intensity of shear localization.

Finally, we examine how damage and energy partitioning are manifest in the net measurable energy budget and exchange of energy between deformational work, heating and interfacial surface energy.

2 BASIC THEORY

Since Bercovici *et al.* (2001a) derived the original two-phase damage theory, we only briefly present the governing equations for the purpose of referencing, but examine those equations being varied in detail. Subscripts f and m refer to fluid and matrix phases, respectively. All dependent variables are not, in fact, true microscopic quantities but are averaged over the fluid or matrix space within small but not necessarily infinitesimal control volumes. Moreover, all equations are invariant to a permutation of subscripts f and m and, implicitly, a switch of ϕ and $1 - \phi$, where ϕ is fluid volume fraction, or porosity; this symmetry property is called 'material invariance' (see Bercovici *et al.* 2001a, for further discussion).

2.1 Mass conservation

The conservation of mass equations are fairly standard in two-phase theories and remain unchanged here. There are two equations involving transport of the fluid and matrix phases:

$$\frac{\partial \phi}{\partial t} + \nabla \cdot [\phi \mathbf{v}_f] = 0 \quad (1)$$

$$\frac{\partial(1 - \phi)}{\partial t} + \nabla \cdot [(1 - \phi) \mathbf{v}_m] = 0, \quad (2)$$

where \mathbf{v}_f and \mathbf{v}_m are the fluid and matrix velocities. Eqs (1) and (2) can be added to yield a continuity equation

$$\nabla \cdot \bar{\mathbf{v}} = 0, \quad (3)$$

where the average and difference of any quantity q are defined as

$$\bar{q} = \phi q_f + (1 - \phi) q_m, \quad \Delta q = q_m - q_f, \quad (4)$$

respectively.

2.2 Momentum conservation

The momentum or force balance equations involve surface tension forces and are thus the first set of equations to be varied, so we will present their derivation more thoroughly.

As shown in Bercovici *et al.* (2001a), the force balance on the fluid phase, averaged over the fluid volume, leads to

$$0 = -\nabla[\phi P_f] + \nabla \cdot [\phi \underline{\tau}_f] - \rho_f \phi g \hat{\mathbf{z}} + \mathbf{h}_f, \quad (5)$$

where P_f is the pressure averaged over the fluid volume, $\underline{\tau}_f$ is the viscous stress tensor averaged over the fluid volume, ρ_f is the density of the fluid phase (assumed constant), g is gravity, and \mathbf{h}_f is the interaction force which results from forces acting on the fluid

across its interface with the matrix. A similar development for the matrix results in

$$0 = -\nabla[(1 - \phi)P_m] + \nabla \cdot [(1 - \phi)\underline{\tau}_m] - \rho_m(1 - \phi)g\hat{\mathbf{z}} + \mathbf{h}_m \quad (6)$$

where P_m and $\underline{\tau}_m$ are the average pressure and stress in the matrix, ρ_m the matrix density (also constant) and the interaction force \mathbf{h}_m results from forces acting on the matrix across its interface with the fluid. The fluid and matrix deviatoric stresses are given by

$$\underline{\tau}_j = \mu_j \left[\nabla \mathbf{v}_j + [\nabla \mathbf{v}_j]^t - \frac{2}{3}(\nabla \cdot \mathbf{v}_j)\underline{\mathbf{I}} \right] \quad (7)$$

where $j = f$ or m , and μ_j is the true viscosity of phase j (i.e. the viscosity of the phase in its pure form); as discussed by Bercovici *et al.* (2001a) and Ricard *et al.* (2001), we do not explicitly employ the bulk viscosity proposed by McKenzie (1984). Although each phase in its pure form is assumed to have constant viscosity (Bercovici *et al.* 2001a), the factors of ϕ and $1 - \phi$ before $\underline{\tau}_f$ and $\underline{\tau}_m$, respectively, in the mixture force-balance eqs (5) and (6) lead to an effective porosity-dependent viscosity; e.g. in the limit of an inviscid fluid phase, the effective viscosity of the two-phase medium in simple shear is $(1 - \phi)\mu_m$ (Ricard *et al.* 2001).

The total force acting on the entire mixture is given by

$$0 = -\nabla \bar{P} + \nabla \cdot \bar{\underline{\tau}} - \bar{\rho}g\hat{\mathbf{z}} + \nabla(\sigma\alpha) \quad (8)$$

where barred quantities are averaged according to (4), σ is surface tension and

$$\alpha = \alpha_o \phi^a (1 - \phi)^b \quad (9)$$

is the porosity-dependent interfacial area per unit volume in which α_o is a constant with units of m^{-1} , a and b are constants ≤ 1 , and $d\alpha/d\phi$ is the average interface curvature (see Bercovici *et al.* 2001a, for a discussion of the properties of the interface density).

As the sum of (5) and (6) must equal (8), we require that

$$\mathbf{h}_f + \mathbf{h}_m = \nabla(\sigma\alpha), \quad (10)$$

such that without surface tension the interaction forces of the two phases are equal and opposite, i.e. $\mathbf{h}_f = -\mathbf{h}_m$. For a properly determined system (see discussion in Bercovici *et al.* 2001a), we write

$$\mathbf{h}_f = \boldsymbol{\eta} + \omega \nabla(\sigma\alpha) \quad (11)$$

$$\mathbf{h}_m = -\boldsymbol{\eta} + (1 - \omega) \nabla(\sigma\alpha), \quad (12)$$

where $\boldsymbol{\eta}$ is the component of the interaction force that in one phase is equal and opposite to that in the other phase, and ω is the surface energy partitioning function which is presumably between 0 and 1. In Bercovici *et al.* (2001a), we assumed $\omega = \phi$, implying that since the surface tension acts on the common interface between phases, once homogenized by averaging over the mixture, its force acts on each phase equally. Here we relax this heuristic assumption and allow for a more general approach. (Note that we keep the partitioning functions ω and $1 - \omega$ outside the ∇ operators in (11) and (12) since we assume the averaged surface tension forces acting on each phase are parallel to each other, since the true force acts on their common interface.)

As in Bercovici *et al.* (2001a), the simplest form of $\boldsymbol{\eta}$ is given by

$$\boldsymbol{\eta} = c\Delta\mathbf{v} + P^*\nabla\phi, \quad (13)$$

where c is the interfacial drag coefficient (in the limit of $\mu_f \ll \mu_m$ it is equivalent to the Darcy drag coefficient), $\Delta\mathbf{v} = \mathbf{v}_m - \mathbf{v}_f$, $P^* = \theta P_f + (1 - \theta)P_m$ represents a common interfacial pressure, and θ

is some unknown weighting function. To estimate θ we substitute (11)–(13) into (5) and (6), and take the limit of no motion (see Bercovici *et al.* 2001a) which results in

$$(1 - \theta)\Delta P \nabla\phi + \omega\sigma \nabla\alpha = 0, \quad (14)$$

$$\theta\Delta P \nabla\phi + (1 - \omega)\sigma \nabla\alpha = 0, \quad (15)$$

(where $\Delta P = P_m - P_f$) which can both only be true if $\theta = 1 - \omega$; this choice is further verified by the fact that both (14) and (15), along with (9), become the Laplace static equilibrium surface tension condition

$$\Delta P + \sigma \frac{d\alpha}{d\phi} = 0, \quad (16)$$

as should be expected. The general momentum equations for each phase (5) and (6) then become

$$0 = -\phi[\nabla P_f + \rho_f g\hat{\mathbf{z}}] + \nabla \cdot [\phi \underline{\tau}_f] + c\Delta\mathbf{v} + \omega[\Delta P \nabla\phi + \nabla(\sigma\alpha)], \quad (17)$$

$$0 = -(1 - \phi)[\nabla P_m + \rho_m g\hat{\mathbf{z}}] + \nabla \cdot [(1 - \phi)\underline{\tau}_m] - c\Delta\mathbf{v} + (1 - \omega)[\Delta P \nabla\phi + \nabla(\sigma\alpha)]. \quad (18)$$

2.3 Energy conservation and damage

Following the development of Bercovici *et al.* (2001a), the energy equation is separated into two coupled equations representing (1) the evolution of thermal (entropy-related) energy, and (2) the rate of work done on the interface by pressure, surface tension, and viscous deformational work. The interfacial surface energy and the work done by surface tension on the mixture is assumed to be partitioned by the same fraction ω as the surface tension force in the previous section. With these assumptions we arrive at (see Bercovici *et al.* 2001a) for a detailed derivation with the case of $\omega = \phi$)

$$\frac{\overline{D}T}{\rho c} - T \frac{\tilde{D}}{Dt} \left(\alpha \frac{d\sigma}{dT} \right) - T\alpha \frac{d\sigma}{dT} \nabla \cdot \tilde{\mathbf{v}} = Q - \nabla \cdot \mathbf{q} + B \left(\frac{\tilde{D}\phi}{Dt} \right)^2 + (1 - f)\Psi \quad (19)$$

$$\sigma \frac{\tilde{D}\alpha}{Dt} = -\Delta P \frac{\tilde{D}\phi}{Dt} + f\Psi - B \left(\frac{\tilde{D}\phi}{Dt} \right)^2, \quad (20)$$

where T is the temperature (assumed the same in both phases), $-d\sigma/dT$ is the interfacial entropy per unit area (Desjonquères & Spanjaard 1993; Bailyn 1994; Bercovici *et al.* 2001a),

$$\tilde{\mathbf{v}} = \omega \mathbf{v}_f + (1 - \omega) \mathbf{v}_m \quad (21)$$

is the effective velocity of the interface, Q is an intrinsic heat source, \mathbf{q} is an energy flux vector (accounting for heat diffusion and possibly energy dispersion (Bercovici *et al.* 2001a)), and

$$\Psi = c\Delta v^2 + \phi \nabla \mathbf{v}_f : \underline{\tau}_f + (1 - \phi) \nabla \mathbf{v}_m : \underline{\tau}_m \quad (22)$$

(where $\Delta v^2 = \Delta\mathbf{v} \cdot \Delta\mathbf{v}$) is the viscous deformational work, a fraction f of which is partitioned into stored work (in this model stored as interface surface energy) while the remaining part goes toward dissipative heating (Taylor & Quinney 1934; Chrysochoos & Martin 1989); see Bercovici *et al.* (2001a) for further discussion of the partitioning fraction f . The quantity B must be positive, has units of viscosity and the term associated with it represents irreversible viscous work done on pores and grains by the pressure difference

two selvages existing in each phase. If one phase has the larger activation energy, then its selvedge has the larger energy anomaly, and thus that phase contributes a larger fraction of the net surface energy at the interface. In short, the material with larger activation energy likely carries more of the surface energy (i.e. has a more energetic selvedge) than the other phase.

Based on these considerations, we assume that when the surface energy is averaged over the mixture, it is *not* equipartitioned between phases but carried more by the phase with larger activation energy, i.e. surface energy is partitioned between phases according to their molecular bond strengths.

In simple viscous materials, the parameter that quantifies molecular activation energy or bond strength is the viscosity. For example, for either subsolidus or liquid flow, the Eyring model of viscosity predicts that viscosity depends on activation energy according to $\mu \sim e^{\Delta G/kT}$ where k is Boltzman's constant (Bird *et al.* 1960; Turcotte & Schubert 1982). (Only gases have a different viscosity laws, but unlike solids and liquids, gases have neither regular molecular structure nor surface energy.) However, we add the caveat that representing activation energy as a simple function of viscosity is an over-simplification since viscosity depends on other variables such as temperature, composition, grain-size and/or dislocation density. Nevertheless, in a viscous system, information about the activation energy is contained primarily in the viscosity and thus we proceed under the working assumption that they are simple monotonic functions of each other.

We therefore assume that the surface-energy partitioning fraction ω is determined by the phases' activation energy, or alternatively their viscosity. In the limit that the phases' viscosities are equal we assume that the averaged surface energy is equipartitioned, i.e. if $\mu_f = \mu_m$ then $\omega = \phi$, for reasons stated by Bercovici *et al.* (2001a). In general, the simplest relation for ω satisfying these various constraints is

$$\omega = \frac{\phi\mu_f}{\phi\mu_f + (1-\phi)\mu_m}. \quad (30)$$

3.1 The geologically relevant limit of ω and the governing equations

The exact form of the relation for ω is probably not important for many geological applications such as partial melts, and fluids percolating through rock, for which $\mu_f \ll \mu_m$. In these cases, regardless of the relation for ω , we can assume $\omega \approx 0$, which leads to the momentum equations for each phase

$$0 = -\phi[\nabla P_f + \rho_f g \hat{\mathbf{z}}] + c \Delta \mathbf{v}. \quad (31)$$

$$0 = -(1-\phi)[\nabla P_m + \rho_m g \hat{\mathbf{z}}] + \nabla \cdot [(1-\phi)\underline{\boldsymbol{\tau}}_m] - c \Delta \mathbf{v} + [\Delta P \nabla \phi + \nabla(\sigma \alpha)]. \quad (32)$$

Eqs (31) and (32) can be combined to give

$$0 = \nabla[\sigma \alpha - (1-\phi)\Delta P] + \nabla \cdot [(1-\phi)\underline{\boldsymbol{\tau}}_m] - (1-\phi)\Delta \rho g \hat{\mathbf{z}} - \frac{c}{\phi} \Delta \mathbf{v}. \quad (33)$$

The material derivative of ϕ moving with the interface is then related to matrix mass conservation:

$$\frac{\tilde{D}\phi}{Dt} = \frac{D_m\phi}{Dt} = (1-\phi)\nabla \cdot \mathbf{v}_m \quad (34)$$

and the damage eq. (29) becomes

$$\Delta P = -\sigma \frac{d\alpha}{d\phi} + \frac{f^* D_m \phi / Dt}{\gamma + (D_m \phi / Dt)^2} \Psi - \frac{K \mu_m}{\phi(1-\phi)} \frac{D_m \phi}{Dt}, \quad (35)$$

which can be used to eliminate ΔP in (33).

4 LIMITING CASES

The assumption that surface-energy partitioning ω depends on phase viscosity, as suggested in the previous section, can be benchmarked by comparison to two independent limiting cases. One case regarding simple melt transport (McKenzie 1984) does not involve surface energy thus we can test our assumptions about ω even in the case when surface energy σ is zero.

4.1 Melt transport and compaction: McKenzie (1984)

The application of two-phase physics to problems of magma dynamics is perhaps best known through the work of McKenzie (1984, 1985, 1987) (see also McKenzie & Holness 2000). Aside from damage and interface thermodynamics, the greatest difference between the theories of McKenzie (1984) and Bercovici *et al.* (2001a) is that Bercovici *et al.* (2001a) adheres to material invariance and does not invoke the McKenzie (1984) assumption of a matrix bulk viscosity. Both Bercovici *et al.* (2001a) and Ricard *et al.* (2001) discussed the correspondence and disagreement between these two theories. We show here, however, that the correspondence between these two theories becomes exact in the proper limits and given the above considerations of the partitioning fraction ω .

The McKenzie (1984) theory assumes constitutive laws for each phase of the form

$$\underline{\boldsymbol{\sigma}}_f = -P \mathbf{I} \quad (36)$$

$$\underline{\boldsymbol{\sigma}}_m = -P \mathbf{I} + \eta (\nabla \mathbf{v}_m + [\nabla \mathbf{v}_m]^T) + \left(\zeta - \frac{2}{3} \eta \right) \nabla \cdot \mathbf{v}_m \mathbf{I} \quad (37)$$

where $\underline{\boldsymbol{\sigma}}_j$ is the full stress tensor of phase j ; P is the fluid pressure; η is the effective matrix viscosity; and ζ is the matrix bulk viscosity. These constitutive laws allow a non-null solution in the case of isotropic compaction, where each phase is exposed to a different isotropic compressive stress, say $-\Pi_f$ and $-\Pi_m$, such that

$$\frac{1}{3} \text{Tr}(\underline{\boldsymbol{\sigma}}_f) = -P = -\Pi_f \quad (38)$$

$$\frac{1}{3} \text{Tr}(\underline{\boldsymbol{\sigma}}_m) = -P + \zeta \nabla \cdot \mathbf{v}_m = -\Pi_m \quad (39)$$

Thus

$$\zeta \nabla \cdot \mathbf{v}_m = -\Delta \Pi, \quad (40)$$

which implies that if $\Pi_m > \Pi_f$ the matrix is squeezed more than the fluid and thus the matrix is compacted. Alternatively, if the entire mixture undergoes uniform isotropic compressive stress such that $\Pi_m = \Pi_f$, then there is no compaction ($\nabla \cdot \mathbf{v}_m = 0$) which therefore preserves the incompressibility of the mixture of two incompressible fluids (i.e. both McKenzie 1984; Bercovici *et al.* 2001a, assume the mixture is composed of constant density fluids).

With the bulk-viscosity approach it is necessary to assume that $\zeta \rightarrow \infty$ as $\phi \rightarrow 0$ (Schmeling 2000; Ricard *et al.* 2001), otherwise, with constant ζ , compaction is predicted to proceed even after $\phi = 0$, which is nonphysical. Moreover, as discussed in Bercovici *et al.* (2001a), it is not possible to extend the bulk-viscosity approach to obtain a materially invariant theory.

The Bercovici *et al.* (2001a) theory, alternatively, obtains a materially invariant set of equations and avoids the bulk viscosity assumption; however, the form presented by Bercovici *et al.* (2001a) has certain failings of its own that we address here. In particular,

the full stress tensors for each phase in the Bercovici *et al.* (2001a) theory are given by

$$\underline{\sigma}_f = -P_f \mathbf{I} + \mu_f \left(\nabla \mathbf{v}_f + [\nabla \mathbf{v}_f]^\dagger - \frac{2}{3} \nabla \cdot \mathbf{v}_f \mathbf{I} \right) \quad (41)$$

$$\underline{\sigma}_m = -P_m \mathbf{I} + \mu_m \left(\nabla \mathbf{v}_m + [\nabla \mathbf{v}_m]^\dagger - \frac{2}{3} \nabla \cdot \mathbf{v}_m \mathbf{I} \right). \quad (42)$$

In the same limit of isotropic compaction discussed above we obtain

$$\frac{1}{3} \text{Tr}(\underline{\sigma}_f) = -P_f = -\Pi_f \quad (43)$$

$$\frac{1}{3} \text{Tr}(\underline{\sigma}_m) = -P_m = -\Pi_m, \quad (44)$$

which leads to $\Delta P = \Delta \Pi$. For consistency with McKenzie (1984), we assume no damage or surface energy ($f = \sigma = 0$), and $\mu_f \ll \mu_m$ and obtain from (29)

$$\Delta \Pi = \Delta P = -\frac{K \mu_m}{\phi(1-\phi)} [(1-\omega)(1-\phi) \nabla \cdot \mathbf{v}_m - \omega \phi \nabla \cdot \mathbf{v}_f] \quad (45)$$

where, even though $\mu_f \ll \mu_m$, we have momentarily retained the general dependence on ω for the sake of discussion.

If ϕ is uniform, the choice of ω is irrelevant; in that case (3) implies $\phi \nabla \cdot \mathbf{v}_f = -(1-\phi) \nabla \cdot \mathbf{v}_m$ and the dependence on ω in (45) vanishes. However, if ϕ is not uniform, and we adopt the assumption of Bercovici *et al.* (2001a) that $\omega = \phi$, we obtain the non-intuitive result that compaction depends on fluid velocity even though the fluid is assumed relatively inviscid (and the fluid can, of course, obtain very high velocities relative to the matrix). Thus, we can best assure a physical solution by assuming that $\omega \rightarrow 0$ as $\mu_f/\mu_m \rightarrow 0$. This inference of the behaviour of ω with phase viscosity is deduced completely independently of the surface energy considerations presented in Section 3 (since surface energy is zero in the comparison to the McKenzie 1984 theory). Therefore we see at least two separate lines of reasoning pointing to ω depending on μ_f and μ_m .

Thus, adopting the assumption that $\omega \approx 0$ in the limit $\mu_f \ll \mu_m$, the compaction condition (45) becomes

$$\frac{K \mu_m}{\phi} \nabla \cdot \mathbf{v}_m = -\Delta \Pi, \quad (46)$$

which is a simpler, physically self-consistent condition that precludes compaction beyond $\phi = 0$. Therefore, allowing for $\omega \rightarrow 0$ as $\mu_f/\mu_m \rightarrow 0$ exactly recovers the McKenzie (1984) theory (i.e. compare 40 and 46) assuming that $\zeta = K \mu_m/\phi$ which, as mentioned above, is desirable anyway.

Therefore, accounting for a surface energy partitioning ω that depends on phase viscosity (or activation energy) allows us to both preserve the general material invariance of the Bercovici *et al.* (2001a) theory while at the same time exactly recovering (and completing the correspondence with) the McKenzie (1984) theory. That both theories match at the relevant limit of $\mu_f \ll \mu_m$ provides them at least some partial validation.

4.2 Void theory: Ricard & Bercovici (submitted.)

Ricard & Bercovici (submitted.) have proposed a variant of the two-phase damage theory in which the pores are evacuated voids. In this case, the pores have zero density, pressure and viscosity ($\rho_f = P_f = \mu_f = 0$). At the interface there is no interaction force between phases ($c \Delta v = 0$) and the interface itself is assumed to move with the matrix. In this limit, as Ricard & Bercovici (submitted.) show,

the governing equations of mass, momentum and surface energy (damage) are, respectively,

$$\frac{\partial \phi}{\partial t} = \nabla \cdot [(1-\phi) \mathbf{v}_m] \quad (47)$$

$$0 = \nabla [\sigma \alpha - (1-\phi) P_m] + \nabla \cdot [(1-\phi) \underline{\tau}_m] - (1-\phi) \rho_m g \hat{\mathbf{z}} \quad (48)$$

$$P_m = -\sigma \frac{d\alpha}{d\phi} + \frac{f^* D_m \phi / Dt}{\gamma + (D_m \phi / Dt)^2} \Psi - \frac{K \mu_m}{\phi(1-\phi)} \frac{D_m \phi}{Dt} \quad (49)$$

(where Ψ is as defined in 22 but with $c \Delta v^2 = 0$) which leads to a simpler set of equations than the full two-phase theory since the fluid velocity \mathbf{v}_f is eliminated. These equations are derived from integral conservation laws independent of assumptions about surface energy partitioning ω since there is no matter in the pores to which the surface energy can be partitioned; the surface energy, by nature of the ‘void’ assumption, must reside entirely in the matrix.

With the dependence of ω on viscosity proposed in Section 3 (and inferred independently in Section 4.1), the void limit ($\rho_f = P_f = \mu_f = c \Delta v = 0$) leads to $\omega = 0$, and we find an exact correspondence between the void eqs (47)–(49) and the two-phase eqs (2), (33) and (35), assuming $\phi \neq 0$. This was not the case with the original Bercovici *et al.* (2001a) version of theory in which $\omega = \phi$.

Therefore, allowing a dependence of ω on phase viscosity permits an exact correspondence between the general two-phase theory and the McKenzie (1984) magma-dynamics theory in the limit $\mu_f \ll \mu_m$, as well as the Ricard & Bercovici (submitted.) theory in the evacuated-void limit.

5 1-D THEORY FOR SHEAR LOCALIZATION AND DEFORMATIONAL WORK PARTITIONING

Here we examine one-dimensional (1-D) shear calculations similar to those used in Bercovici *et al.* (2001b). We find that assuming $\omega = 0$ for $\mu_f \ll \mu_m$, instead of $\omega = \phi$, has little overall effect on the 1-D calculations, although the resulting theory permits an improved analytic understanding of the nonlinear results. We also use the 1-D theory to further examine the role of partitioning of deformational work between damage (energy stored on the interface as surface energy) and dissipation.

5.1 1-D equations

Our domain is infinitely long in the x direction and is $2L$ wide, going from $y = -L$ to $+L$. The boundaries are impermeable and no slip and move in the x direction with equal and opposite velocities of magnitude V_x ; thus at $y = \pm L$, $v_{m_x} = v_{f_x} = \pm V_x$ and $v_{m_y} = v_{f_y} = 0$. All dependent variables depend only on y and time t . Because the system is 1-D and the boundaries at $y = \pm L$ are rigid (i.e. $v_{m_y} = v_{f_y} = 0$ at the boundaries) the continuity eq. (3) becomes

$$\phi v_{f_y} + (1-\phi) v_{m_y} = 0 \quad (50)$$

and thus if $\phi \neq 0$ we obtain

$$\Delta v_y = v_{m_y} / \phi. \quad (51)$$

In 1-D, matrix mass conservation (2) yields

$$\frac{\partial \phi}{\partial t} = \frac{\partial}{\partial y} [(1-\phi) v_{m_y}] \quad (52)$$

which we use to define the effective dilation rate

$$\Theta = \frac{D_m \phi}{Dt} = (1 - \phi) \frac{\partial v_{m_y}}{\partial y}. \quad (53)$$

Our layer is assumed to be in the horizontal x - y plane such that gravity does not appear in the relevant force equations. We also assume that $\mu_f \ll \mu_m$ and that the fluid macroscopic stresses are negligible relative to other fluid forces; thus we neglect $\underline{\tau}_f$ but retain interface force terms proportional to $c\Delta v$. Given the formula for c in the limit $\mu_f \ll \mu_m$ (McKenzie 1984; Spiegelman 1993a,b,c; Bercovici *et al.* 2001a), we obtain

$$c = \frac{\mu_f \phi^2}{k_o \phi^n}, \quad (54)$$

where k_o is a reference permeability; adopting the common and simplifying assumption that $n = 2$ (which is really only valid for small porosities), $c = \mu_f/k_o$ is a constant.

With the above assumptions the x component of the fluid force eq. (17) yields $c\Delta v_x = 0$, which implies that $v_{f_x} = v_{m_x}$ throughout the medium. The x component of the matrix force eq. (18) becomes

$$0 = \mu_m \frac{\partial}{\partial y} \left[(1 - \phi) \frac{\partial v_{m_x}}{\partial y} \right] \quad (55)$$

which allows us to define the effective shear rate

$$\Omega = (1 - \phi) \frac{\partial v_{m_x}}{\partial y} = \text{const.} \quad (56)$$

The only equation necessary to describe the force balance in the y direction is (33), which, with (51) and (53), becomes

$$0 = \frac{\partial}{\partial y} \left[\sigma \alpha - (1 - \phi) \Delta P + \frac{4}{3} \mu_m \Theta \right] - c \frac{v_{m_y}}{\phi^2}. \quad (57)$$

The final necessary equation is (35), which, with (22) and our assumptions so far, becomes

$$\Delta P = -\sigma \frac{d\alpha}{d\phi} - \frac{K \mu_m}{\phi(1 - \phi)} \Theta + \frac{f^* \Theta}{\gamma + \Theta^2} \left[c \frac{v_{m_y}^2}{\phi^2} + \frac{\mu_m}{1 - \phi} \left(\Omega^2 + \frac{4}{3} \Theta^2 \right) \right]. \quad (58)$$

Eqs (57) and (58) can be combined to eliminate ΔP and obtain

$$\begin{aligned} \frac{\partial}{\partial y} \left[\sigma(1 - \phi)^2 \frac{d}{d\phi} \left(\frac{\alpha}{1 - \phi} \right) + \mu_m \left(\frac{4}{3} + \frac{K}{\phi} - f^* \frac{\Omega^2 + \frac{4}{3} \Theta^2}{\gamma + \Theta^2} \right) \Theta \right] \\ = c \left[\frac{v_{m_y}}{\phi^2} + f^* \frac{\partial}{\partial y} \left(\frac{(1 - \phi) \Theta v_{m_y}^2}{\phi^2 (\gamma + \Theta^2)} \right) \right]. \end{aligned} \quad (59)$$

We must also treat the special case of $\phi = 0$ (since, for example, the final force eq. (59) is only valid for $0 < \phi < 1$). In this case, and given our assumptions so far, (3) becomes $\Delta v_y \partial \phi / \partial y = \partial v_{m_y} / \partial y$. However, since $\phi = 0$ is the minimum value of ϕ , $\partial \phi / \partial y = 0$ when $\phi = 0$, and thus $\partial v_{m_y} / \partial y = 0$; also, with the rigid boundaries, $v_{m_y} = 0$ when $\phi = 0$. These two constraints on v_{m_y} lead to $\partial \phi / \partial t = 0$ (from 52). These relations would then replace (52) and (59) as the relevant equations for the case $\phi = 0$. Similar conditions exist for the case $\phi = 1$, assuming that our basic approximations (e.g. that $\underline{\tau}_f$ is negligible) are applicable in this limit.

5.1.1 Nondimensionalization

Assuming σ is constant, and making the substitutions $y = Ly'$, $\alpha = \alpha_0 \alpha'$

$$\left(\Theta, \Omega, \frac{v_{m_y}}{L}, \sqrt{\gamma}, 1/t \right) = \frac{\sigma \alpha_0}{\mu_m} \left(\Theta', \Omega', \frac{w}{L}, \sqrt{\gamma'}, 1/t' \right) \quad (60)$$

our governing equations become (dropping the primes)

$$\frac{\partial \phi}{\partial t} = \frac{\partial(1 - \phi)w}{\partial y} \quad (61)$$

$$\begin{aligned} \frac{\partial}{\partial y} \left[(1 - \phi)^2 \frac{d}{d\phi} \left(\frac{\alpha}{1 - \phi} \right) + \left(\frac{4}{3} + \frac{K}{\phi} - \frac{\nu + \frac{4}{3} f^* \Theta^2 / \gamma}{1 + \Theta^2 / \gamma} \right) \Theta \right] \\ = \lambda \left[\frac{w}{\phi^2} + f^* \frac{\partial}{\partial y} \left(\frac{(1 - \phi) \Theta w^2 / \gamma}{\phi^2 (1 + \Theta^2 / \gamma)} \right) \right], \end{aligned} \quad (62)$$

where

$$\Theta = (1 - \phi) \frac{\partial w}{\partial y} \quad (63)$$

$$\lambda = \frac{cL^2}{\mu_m} \quad (64)$$

$$\nu = f^* \Omega^2 / \gamma \quad (65)$$

and now

$$\alpha = \phi^a (1 - \phi)^b. \quad (66)$$

The parameter ν , as discussed by Bercovici *et al.* (2001b), represents the amount of stored deformational work done by the shear stress imposed on the layer.

6 LINEAR STABILITY ANALYSIS

The stability of the system to perturbations is in fact identical to that presented by Bercovici *et al.* (2001b). To demonstrate this one simply substitutes for our dependent variables a constant background state plus a perturbation

$$\begin{aligned} \phi &= \phi_0 + \epsilon \phi_1(y, t) \\ w &= \epsilon w_1(y, t) \end{aligned} \quad (67)$$

$$\Theta = \epsilon \Theta_1 = \epsilon (1 - \phi_0) \frac{\partial w_1}{\partial y}$$

where $\epsilon \ll 1$ and because of the rigid impermeable boundaries the background state of order ϵ^0 for w and Θ must be zero to conserve mass. Placing these in the standard way into our governing eqs (61) and (62), and assuming all terms of order ϵ^1 go as e^{iky+st} , then the growth rate s of a perturbation of wavelength $2\pi/k$ is given by

$$s = \frac{G(\phi_0)k^2}{\phi_0(1 - \phi_0)[K + \phi_0(4/3 - \nu)]k^2 + \lambda} \quad (68)$$

where

$$\begin{aligned} G(\phi) &= -\phi^2(1 - \phi)^2 \frac{d^2 \alpha}{d\phi^2} \\ &= \phi^a(1 - \phi)^b \{a(1 - a) + (a + b - 1)[2a - (a + b)\phi]\}. \end{aligned} \quad (69)$$

As discussed in Ricard *et al.* (2001) and Bercovici *et al.* (2001b), $G(\phi) > 0$ for all porosities. Thus, the growth rate s is positive for no shear or damage ($\nu = 0$), which reflects the instability of the system to surface-tension driven segregation of the two phases, termed 'self-separation'; this effect is due to the tendency of surface tension to minimize interfacial area, thereby unmixing the two phases

(much as oil floating on the surface of water). The influence of damage and shear on the growth rate s is only evident in the parameter ν . Damage and shear increase the growth rate as long as $\nu < 4/3 + K/\phi_0$ which suggest that damage accelerates phase separation into a rapidly growing localization. Otherwise, for larger ν , damage effects can cause negative growth rates which are interpreted as inhibition of localization and distributed damage. Discussion of the linear stability results are discussed more fully in Ricard *et al.* (2001) and Bercovici *et al.* (2001b).

7 NON-LINEAR SOLUTIONS: LOCALIZATION AND THE EFFECT OF WORK-PARTITIONING VARIABILITY

As shown in Ricard *et al.* (2001) and Bercovici *et al.* (2001b), spontaneous separation of the phases (self-separation) occurs when there is no shear or damage ($\nu = 0$). Non-linear solutions in this limit are demonstrated in Fig. 1(a), showing smooth and well-rounded porosity profiles collapsing in width and growing in amplitude with increasing time. However, with damage and shear, a variety of effects ensue, as discussed below.

7.1 An apparent singular point

Much of the localization effects occurring with damage can be understood upon inspection of the force eq. (62). In particular, for Θ^2/γ very small, eq. (62) has an apparent singular point (an irregular singular point, to be precise (Bender & Orszag 1978)) at values of y where $\phi = K/(\nu - 4/3)$. By definition, Θ itself would be singular at this point, thus leading to an infinitely fast growth rate in ϕ and thus an extreme localization. (This is related to the apparent infinite growth rate given by (68) in the linear analysis when $\phi_0 = K/(\nu - 4/3)$; however, the existence of the apparent singular point discussed here is relevant for all porosity fields, whereas the linear analysis only applies to porosity fields that are constant to 0th order.) We refer to this only as an ‘apparent’ singular point because, once Θ grows toward a singularity, Θ^2/γ is obviously no longer negligible and the singular point, in effect, ceases to exist. The singular point is, thus, only apparent as long as Θ^2/γ is small, and therefore the singularity in Θ —and thus a singular localization in ϕ —is self-limiting. Nevertheless, we can use the concept of the apparent singular point to extract important information from the system.

7.2 Weak localization

Since ϕ can never exceed 1, the apparent singular point does not exist if $K/(\nu - 4/3) > 1$, or $\nu < K + 4/3$. In this case, Θ can never approach a near-singularity within the allowable range of ϕ . Values of ν less than $K + 4/3$ therefore define the *weak localization* regime—or what Bercovici *et al.* (2001b) referred to as the ‘accelerated separation regime’. In this regime, shear and damage enhance the generation of a high porosity weak zone (which occurs anyway under surface-tension driven self-separation; Fig. 1a), but they do not drastically sharpen the profiles in porosity ϕ or transverse velocity w (Fig. 1b).

7.3 Strong localization

For $\nu > K + 4/3$ the apparent singular point can exist and sharpened profiles are allowed. This range of ν corresponds to strong

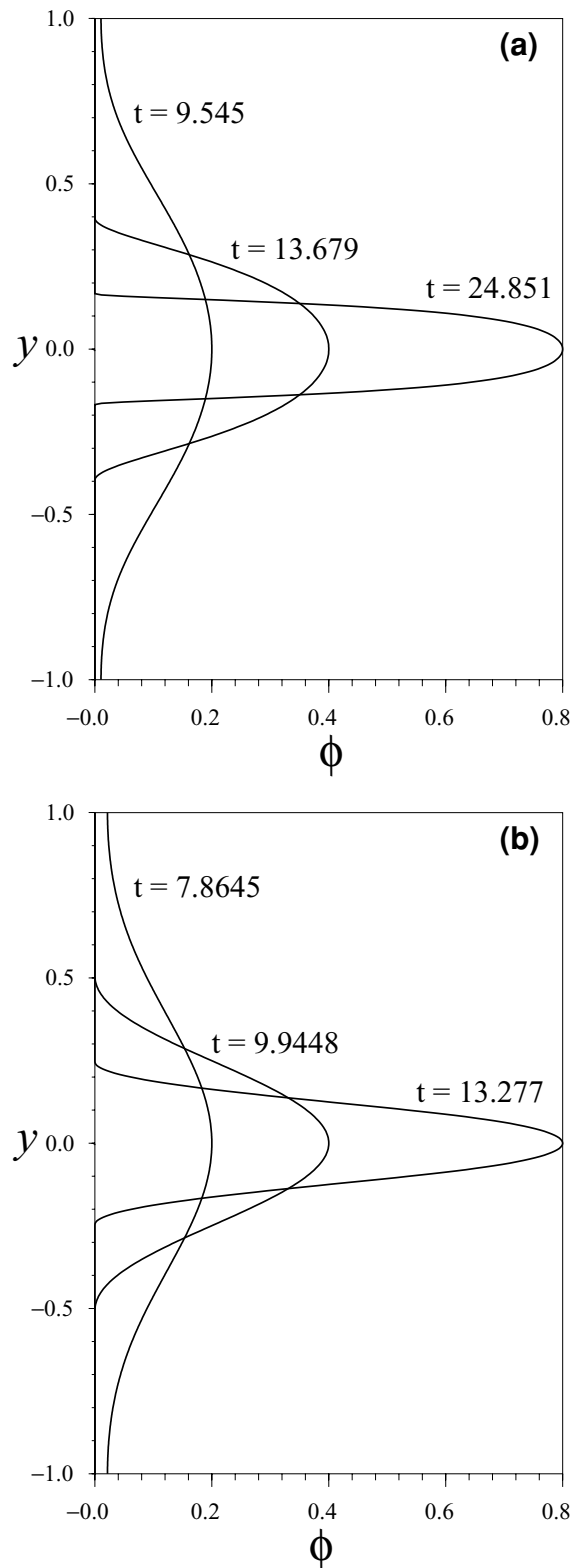


Figure 1. Profiles of porosity ϕ for different times (values indicated) and two values of ν . In all cases $K = 1$, $f^* = 0.1$, $\gamma = 100$, $a = b = 0.5$, $\lambda = 0$. With $\Omega^2 = \nu = 0$ (a) there is no influence of shear and damage and the fluid and matrix segregate by surface-tension driven self separation; this is shown for the sake of comparison. For the $\nu = 2$ ($\Omega^2 = 2000$) case (b), there is influence from shear and damage both morphologically and in the rate of separation of the phases; however, localization is weak since $\nu < K + 4/3$ (see text for discussion).

localization, or what Bercovici *et al.* (2001b) referred to as the ‘tear localization’ regime. However, as stated above, the effect of the apparent singularity is self-limiting; as Θ becomes large enough the non-linear terms on the left of (62) mitigate the apparent singularity, and thus preclude a truly singular Θ , and discontinuously sharp ϕ (Fig. 2b).

Yet, in this regard, the role of variability in deformational-work partitioning, represented by the parameter γ , is very important, in particular the case with $\gamma \gg 1$. For large γ it is obviously more difficult for the system to achieve the maximum partitioning of deformational work toward damage and creation of surface energy. Thus, to achieve the same basic effect as with a smaller γ , one must impose a larger shear stress Ω ; i.e. to obtain the same growth rates and apparent singular points, one needs to hold ν constant, and thus increase $f^*\Omega^2$ in proportion to γ . However, the larger γ also suppresses the non-linear terms that mitigate the apparent singular point; i.e. Θ must become very large before the singularity is mitigated, and can, in fact, become almost singular (obviously, in the limit $\gamma \rightarrow \infty$, Θ would need to become singular before having any mitigating effect on the system, by which point it is too late to do so). Thus, strong localization can only occur for $\nu > K + 4/3$, and is most pronounced for large γ (Fig. 2c). However, the growth rates are still predominantly dependent only on ν (compare times in Figs 2b and c), even if the morphologies of the localizations are significantly different.

7.4 Distributed damage

As predicted by linear stability analysis (see 68), when ν is large enough such that the entire porosity field initiates with $\phi > K/(\nu - 4/3)$, then defocusing or distributed damage can occur, and porosity anomalies decay away rather than localize (Fig. 3). This is interpreted by Bercovici *et al.* (2001b) to mean that once beyond this critical state, the energy input from deformational work is too large to be accommodated by a growing localization, and thus the entire system is damaged.

However, to some extent, distributed damage solutions require certain conditions which are best illustrated by taking the limit of $\lambda = 0$, and integrating (62) in y to obtain

$$\left[\frac{4}{3} + \frac{K}{\phi} - \nu + \left(\frac{4}{3}(1 - f^*) + \frac{K}{\phi} \right) \frac{\Theta^2}{\gamma} \right] \Theta = \Gamma \left(1 + \frac{\Theta^2}{\gamma} \right) \quad (70)$$

where

$$\Gamma = \Sigma - (1 - \phi)^2 \frac{d}{d\phi} \left(\frac{\alpha}{1 - \phi} \right) \quad (71)$$

and Σ is an integration constant determined by the boundary conditions $w = 0$ at $y = \pm 1$, or alternatively $\int_{-1}^{+1} \frac{\Theta}{1 - \phi} dy = 0$. (This system is also very similar to that explored in the evacuated-void limit by Ricard & Bercovici (submitted) and is discussed in more detail there.)

When the entire porosity field satisfies $\phi > K/(\nu - 4/3)$, as many as three real roots to (70) can exist, in particular, two large $|\Theta|$ roots (of opposite sign), and one small $|\Theta|$ root (Fig. 4). The large- $|\Theta|$ solutions can be realized if the system is initiated with large enough local dilation and compaction rates. In order that the system satisfy mass conservation in the confined layer (i.e. $\int_{-1}^{+1} \frac{\Theta}{1 - \phi} dy = 0$) a combination of the two large $|\Theta|$ roots (one positive and one negative) is required so that dilation of the matrix in one part of the layer is compensated by compaction elsewhere. Since the two large $|\Theta|$ roots are not connected, the overall solution combining the two entails a discontinuity in Θ which requires special matching

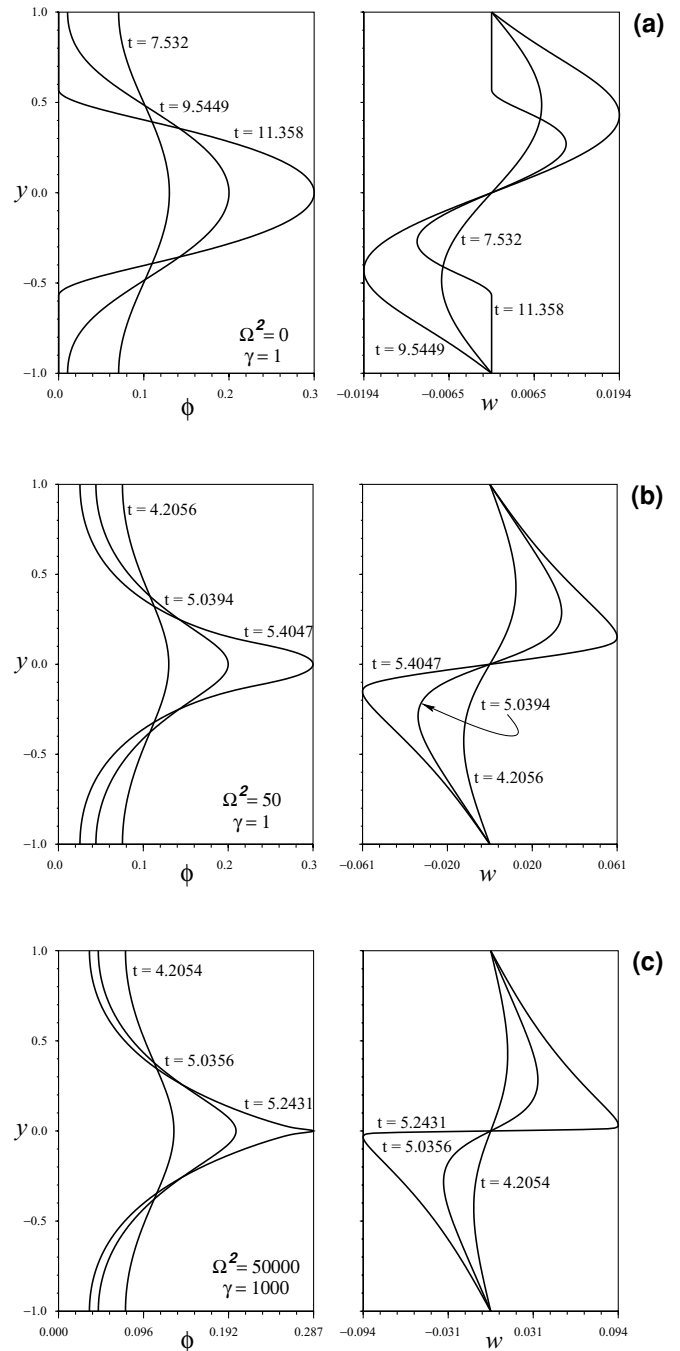


Figure 2. Profiles of porosity ϕ and transverse velocity w for different times (as indicated) and parameter values Ω and γ (also indicated). In all cases $K = 1$, $f^* = 0.1$, $a = b = 0.5$, $\lambda = 0$. Evolution of the system for no shear stress $\Omega = 0$, and thus only surface-tension driven self-separation, is shown for comparison (a). Frames (b) and (c) show the system for the same value of $\nu = 5$, but different values of γ as indicated (thus Ω^2 is changed in proportion to γ). Since $\nu > K + 4/3$ an apparent singular point is allowed, but not necessarily realized since non-linear terms can mitigate the singularity if γ is of order unity (b). However, if $\gamma \gg 1$ this mitigation effect is suppressed leading to a nearly discontinuous profiles in velocity w (thus a nearly singular $\Theta = (1 - \phi) \frac{\partial w}{\partial y}$) and a sharp localization in porosity (c).

conditions in numerical analysis. Such a system initiated with $\Theta < 0$ for $\phi < \phi^*$ and $\Theta > 0$ for $\phi > \phi^*$ (where ϕ^* is the porosity at which the discontinuity in Θ occurs) is unstable and will undergo localization; i.e. regions with porosities less than ϕ^* will compact

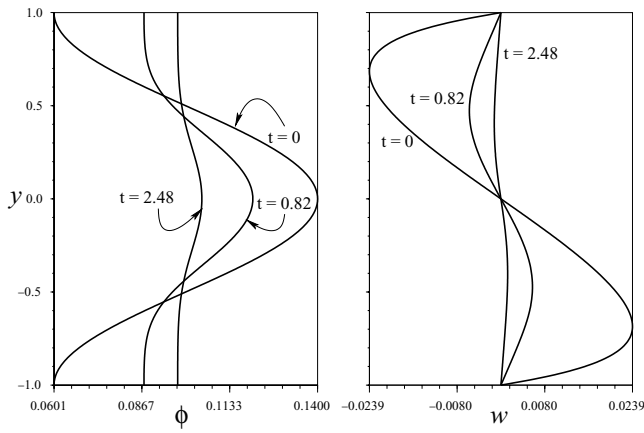


Figure 3. Profiles of porosity ϕ and transverse velocity w for different times (values indicated) and large ν . In this case $\Omega^2 = 200$, $K = 1$, $f^* = 0.1$, $\gamma = 1$, $a = b = 0.5$, $\lambda = 0$. Thus, the value of ν is 20. This figure shows the behaviour of the system for ‘delocalization’ and distributed damage, wherein shear and damage cause a porosity anomaly to decay, effectively mixing the phases, even with an initial finite-amplitude porosity perturbation.

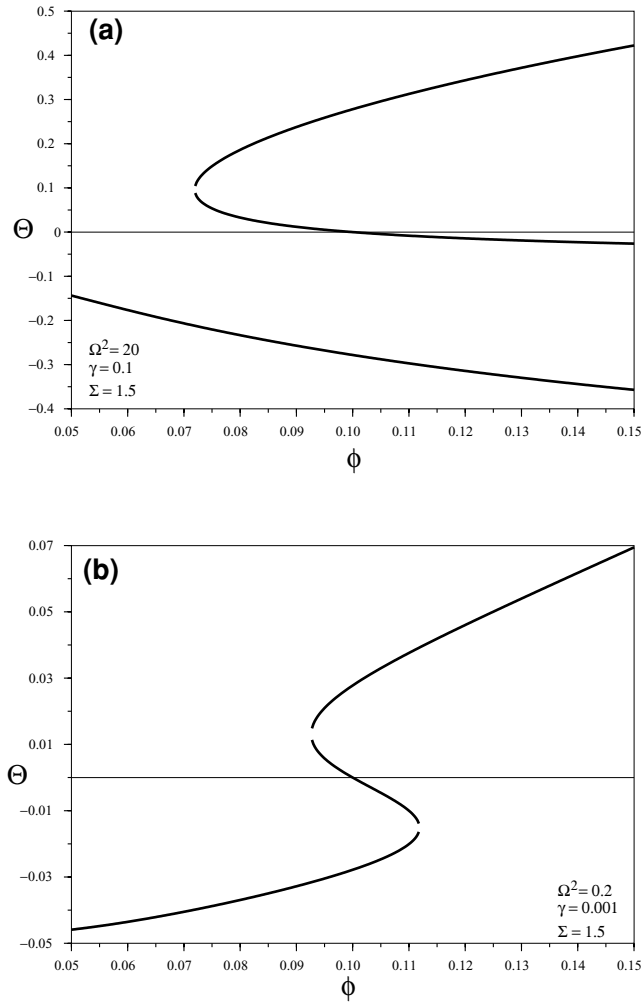


Figure 4. Solutions of Θ versus ϕ from (70). Here $\nu = f^*\Omega^2/\gamma$ is held fixed at 20, although γ is varied as indicated. Otherwise, $K = 1$, $f^* = 0.1$, $a = b = 0.5$, $\lambda = 0$. Σ is chosen so that an equilibrium solution $\Theta = 0$ exists at $\phi = 0.1$; this requires—by (70) and (71)—that $\Gamma = 0$ at $\phi = 0.1$, and thus (given the values of a and b) $\Sigma = 1.5$.

and ϕ will decay to 0, while those with porosities greater than ϕ^* will dilate and ϕ will grow to 1.

If the system is initiated at or near rest, then it will tend toward the small $|\Theta|$ root since (for the situation in which $\phi > K/(\nu - 4/3)$) this is the only branch of solutions that contains the rest-solution $\Theta = 0$ (Fig. 4). The rest solution is stable because, if $\Theta = 0$ at $\phi = \phi_0$, then portions of the layer with $\phi < \phi_0$ have $\Theta > 0$ and undergo dilation to a state where $\phi = \phi_0$, while portions with $\phi > \phi_0$ have $\Theta < 0$ and will compact to $\phi = \phi_0$ (see Fig. 4). Since this solution involves forcing the system toward a uniform porosity it is associated with distributed damage.

However, as illustrated in Fig. 4(b), the small $|\Theta|$ root does not exist for all ϕ , and in fact exists for only a narrow range of ϕ if γ is very small. In particular, the small $|\Theta|$ solutions correspond to the condition $\Theta^2/\gamma \ll 1$, which with (70) leads to

$$\Theta \approx \frac{\Gamma}{4/3 + K/\phi - \nu}, \tag{72}$$

however, (72) is in itself only consistent with $\Theta^2/\gamma \ll 1$ if

$$\left| \frac{\Gamma}{4/3 + K/\phi - \nu} \right| \ll \sqrt{\gamma}. \tag{73}$$

As $\gamma \rightarrow 0$ (holding ν fixed in order to keep the basic growth rate constant), (73) is only satisfied for Γ close to zero; yet, since the function $\Gamma = 0$ at only one porosity, say, $\phi = \phi_\Gamma$ (e.g. using 9, 71, and $a = b = 1/2$, $\phi_\Gamma = (1 + 4\Sigma^2)^{-1}$), then (73) will only hold for ϕ sufficiently close to ϕ_Γ . Thus, in the end, there is only a narrow range in ϕ over which the small- Θ solutions exist when $\gamma \ll 1$ (Fig. 4b). If the system is initiated at or near rest with porosities outside this range, the system will be forced toward a discontinuous combination of the large $|\Theta|$ solutions which thus entails instability and localization. (Alternatively, if $\gamma \rightarrow 0$ but $f^*\Omega^2$ is fixed, then $\nu \rightarrow \infty$, thereby automatically satisfying (73) and allowing small- Θ solutions to exist for nearly all $\phi > K/(\nu - 4/3)$.)

Physically, the above analysis implies that distributed damage can occur if the magnitude of the shear stress $|\Omega|$ exceeds a critical value given by

$$\Omega_c = \sqrt{\frac{\gamma}{f^*} \left(\frac{4}{3} + \frac{K}{\phi} \right)}. \tag{74}$$

For smaller work-partitioning variability γ , a smaller shear stress is required to achieve the maximum work partitioning necessary to cause such wide-scale damage. However as $\gamma \rightarrow 0$ a vanishingly small shear stress Ω can still cause distributed damage, but only in the vicinity of porosities where normal stress and surface-tension forces are precariously balanced, i.e. near where $\Gamma = 0$. Outside this vicinity of porosities, the effect due to the difference between normal stress and surface tension forces is more significant than damage due to shear stress, and thereby either dilation of matrix with larger porosities or compaction of matrix with smaller porosities occurs (depending on the sign of Γ) leading to amplification of porosity anomalies, localization and phase-separation instead of defocusing and distributed damage. Therefore, as with the case with strong and sharp localizations, a sufficiently large γ is required to allow distributed damage.

7.5 Localization summary

The occurrence and intensity of localization can be summarized rather succinctly by three regimes whose boundaries are primarily

functions of ν , which represents the shear-work that goes into creating surface energy. In order of increasing ν , these regimes are as follows: (1) for $\nu < K + 4/3$ only weak localization can occur; (2) for $\nu > K + 4/3$, strong localization can occur but is most pronounced for $\gamma \gg 1$; and lastly, (3) distributed (or unlocalized) damage occurs for $\nu > K/\phi_{0\min} + 4/3$, where $\phi_{0\min}$ is the minimum initial porosity (see also other constraints on this regime stated in the previous section).

8 HEAT GENERATION AND ENERGY EXCHANGE

The damage theory used here assumes a certain partitioning, represented by the parameter f , by which some fraction of deformational work is stored as surface energy on the interface. Here, we examine the energy budget of our system to see how the presence of damage is reflected in measurable quantities such as total heat output.

To simplify the energy equation, we assume the heat capacity per volume of the two phases are equal and constant such that $\rho_f c_f = \rho_m c_m = \bar{\rho}c = \text{const.}$, and that internal heat sources, and energy loss by diffusion and dispersion are negligible (i.e. $\mathbf{q} = \mathbf{Q} = 0$). Finally, in keeping with our dimensionless equations, we define the nondimensional temperature

$$\vartheta = \frac{\bar{\rho}c}{\sigma\alpha_o} T. \quad (75)$$

In this way, our thermal energy (entropy- or heat-related) eq. (19) becomes

$$\frac{\partial \vartheta}{\partial t} = \frac{K}{\phi(1-\phi)} \Theta^2 + (1-f) \left(\lambda \frac{w^2}{\phi^2} + \frac{\Omega^2 + \frac{4}{3}\Theta^2}{1-\phi} \right) \quad (76)$$

where the advection term vanishes because of (50). We then use (63) and the integral in y of (62) to obtain

$$\begin{aligned} \frac{\partial \vartheta}{\partial t} = & \frac{\Omega^2}{1-\phi} + \lambda \frac{\partial}{\partial y} \left(w \int \frac{w}{\phi^2} dy \right) \\ & + \left(\Sigma - (1-\phi)^2 \frac{d}{d\phi} \frac{\alpha}{1-\phi} \right) \frac{\Theta}{1-\phi} \end{aligned} \quad (77)$$

where Σ is an integration constant similar to that in (70) and (71). Finally, we integrate across the layer to obtain the total amount of heating; defining

$$\langle X \rangle = \int_{-1}^{+1} X dy \quad (78)$$

where X is any scalar, then from (77) we obtain

$$\langle \dot{\vartheta} \rangle = \frac{d\langle \vartheta \rangle}{dt} = \Omega^2 \langle (1-\phi)^{-1} \rangle - \left\langle \Theta(1-\phi) \frac{d}{d\phi} \frac{\alpha}{1-\phi} \right\rangle \quad (79)$$

where the terms proportional to λ and Σ vanish because $w = 0$ at $y = \pm 1$. (Note, however, that with boundary conditions of $w \neq 0$ at $y = \pm 1$ the term proportional to Σ would represent potentially large deformational work imposed by normal stresses, while the term proportional to λ would represent resistance to net extraction or injection of fluid through the matrix.) We note that in the final bulk heat eq. (79), the partitioning function f , internal dissipation K , and compaction length λ do not appear explicitly; their effect is implicitly in the nature of how they affect the porosity ϕ and dilation rate Θ .

The last term on the right of (79) represents the rate of either release or creation of surface energy since this term can be

either positive or negative. In particular, one can readily show that

$$\left\langle \Theta(1-\phi) \frac{d}{d\phi} \frac{\alpha}{1-\phi} \right\rangle = \left\langle \frac{G(\phi)}{\phi^2(1-\phi)} w \frac{\partial \phi}{\partial y} \right\rangle. \quad (80)$$

When this quantity is negative, surface energy is being released and eventually being dissipated as heat; if positive then surface energy is being created and thus detracts from the net heat output since it necessarily absorbs some of the deformational work. For cases involving phase separation and localization, w and $\frac{\partial \phi}{\partial y}$ are consistently opposite in sign (i.e. 180° out of phase), as can be seen by inspection of Fig. 2; thus, since $G(\phi) > 0$, the quantity in (80) is negative and surface energy is being released during localization, although the rate of this release is modulated by damage and shear as discussed below. In the case of distributed damage, w and $\frac{\partial \phi}{\partial y}$ are consistently of the same sign (i.e. in phase) as can be inferred from Fig. 3, and thus surface energy is being created as the phases become more thoroughly mixed; the net entropy production in (79) is thus reduced, but necessarily remains positive since distributed damage only occurs for large Ω^2 .

However, in this system (with rigid boundaries) Θ is at most a 1st order variable and the last term on the right of (79) is necessarily 2nd order while the first term is 0th order, unless an unusually small Ω is used. (This can be seen by using the expansions given by (67) in (79) and noting that the integral of terms $O(\epsilon^1)$ are zero.) Thus, the effect of surface energy release or creation on net heat output is in fact extremely small and typically contributes a term with magnitude of the order of 10^{-2} in the dimensionless heating eq. (79). Indeed, as discussed below, the influence that a changing porosity field has on net shear heating $\Omega^2 \langle (1-\phi)^{-1} \rangle$ can be a much more significant effect and overwhelm surface energy release.

In Fig. 5 we display the net heating rate $\langle \dot{\vartheta} \rangle$ and net surface energy $\langle \alpha \rangle$ for sample cases with various values of f^* to show the effect of work-partitioning on the energy budget. For $f^* = 0$ there is obviously no coupling between shear and surface-tension driven separation; the heat generated is simply the sum of imposed deformational work, and the release of surface energy by self-separation as if there were no imposed shear. As f^* increases, shear and damage have an increasing effect on the heat generation. Obviously, the damage process involves transfer of deformational work to interfacial surface energy, and thus one would nominally expect less net dissipative heating in cases with larger maximum work-partitioning f^* . However, the effects of damage on heating and energy exchange are somewhat convoluted and thus warrant some discussion.

In all cases with phase separation and/or localization, with or without damage, the system undergoes loss of net interfacial surface area and energy (e.g. Fig. 5c). Thus even the localizing cases with damage involve a net release—instead of storage—of surface energy. (However, in de-localizing cases with distributed damage, surface energy is increased since the phases desegregate or mix, and thus interfacial area is increased.) In that regard, one might expect cases with damage to retard the release of surface energy and heat relative to cases with lesser or no damage.

However, localizing cases with more damage (i.e. larger work partitioning f^*) also evolve much faster, i.e. the phases separate and the porosity field localizes toward a maximum value faster (Fig. 5a), which causes both terms in (79) (both shear heating and the release rate of surface energy) to become larger, not smaller, with increased damage. Thus at any given time, the cases with larger f^* generate

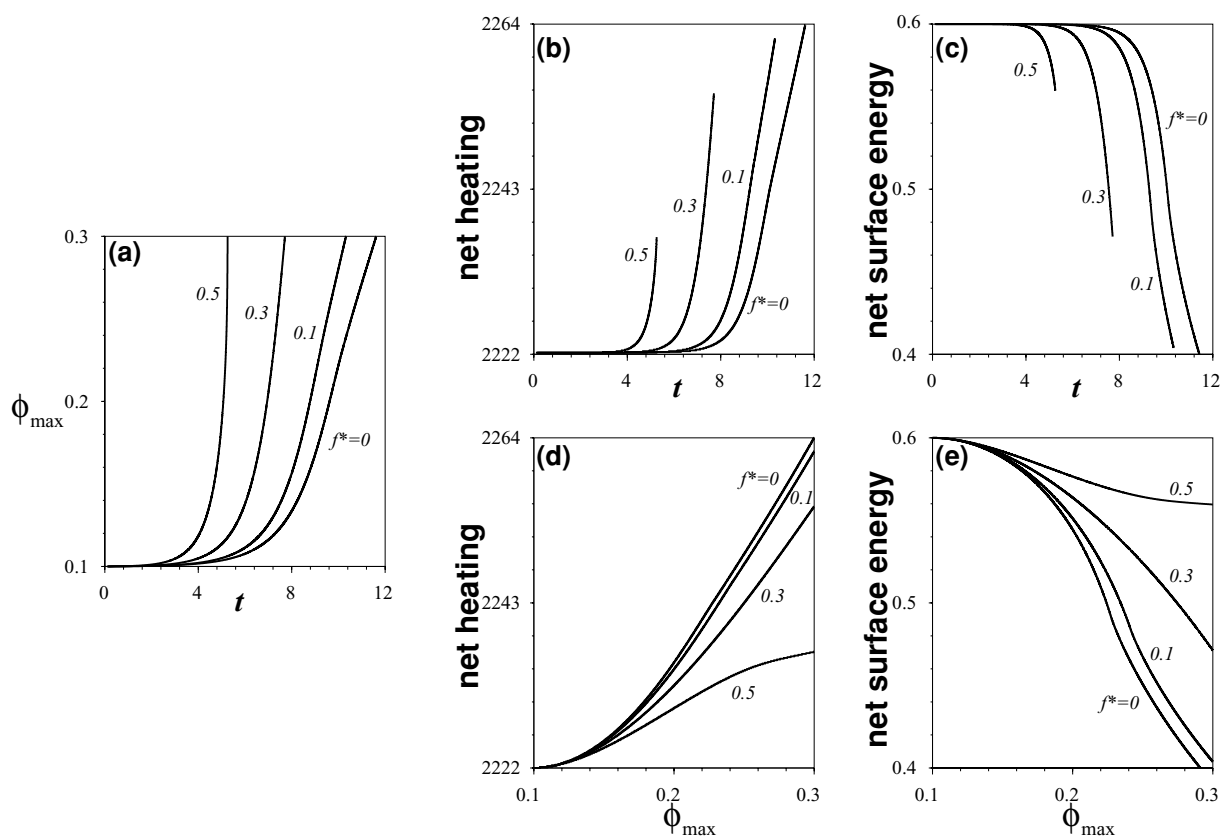


Figure 5. An example of heat generation for cases with $\Omega^2 = 1000$, $\gamma = 100$, and different f^* as indicated; also, for all cases $K = 1$, $a = b = 1/2$, and $\lambda = 0$. First three frames show for each case (a) peak porosity ϕ_{\max} versus time; (b) net heating from (79) versus time; (c) net interfacial surface energy (α) versus time. Since the porosity field evolves on a different timescale for each case, we also depict net heating (d) and interface energy (e) versus peak porosity to show these energies at comparable stages of development.

more heat (Fig. 5b) and have released more surface energy (Fig. 5c). It thus appears that an increase in partitioning of deformational work toward damage (creation of interfacial surface energy) and away from viscous dissipation causes more, not less, viscous heating.

However, because increased partitioning f^* changes the timescale of evolution of the system, in particular making the porosity field localize faster, cases with different f^* are not entirely comparable, unless we compensate for their different developmental timescales. For example, at a given time, a case with large f^* will have reached a larger peak ϕ than with smaller or zero f^* . This causes the amount of deformational work imposed on the system $\Omega^2(1 - \phi)^{-1}$ to be larger; i.e. the shear stress Ω is the same, but the integrated strain rate, or more simply the velocity difference across the layer $\Omega(1 - \phi)^{-1}$ increases with increased peak porosity ϕ_{\max} . Thus while the amount of partitioning is higher for larger f^* cases, the amount of deformational work input into the system is higher, too, causing relatively more heating, as well.

Thus, one should compare the cases with different f^* at equivalent timescales, or more simply at comparable stages of development in the porosity field. For example, when the cases are compared at equivalent peak porosities, the interpretation of energy release changes significantly. In particular, the cases with larger f^* generate less heat (Fig. 5d) and have released less surface energy (Fig. 5e) at a given peak porosity ϕ_{\max} . This shows that at comparable stages of development in the porosity field, cases with larger partitioning

do indeed cause less heating, and release less surface energy. Relative to the unforced system of $f^* = 0$, the $f^* > 0$ cases essentially channel deformational work away from dissipative heating toward surface energy creation (Fig. 6).

The heating and surface-energy for the strongly localizing case (the $f^* = 0.5$ case in Fig. 5, which undergoes a near singularity toward the end of its evolution much like that shown in Fig. 2), appear to plateau with increasing porosity. Thus, the onset of the near singularity appears to correlate with a saturation in heating and surface-energy release.

Although it is not shown, the heating and net surface-energy curves for the distributed damage case shown in Fig. 3 display a simple reversal of curves like those shown in Fig. 5. In particular, the net heating rate simply decreases toward a final value of $2\Omega^2/(1 - \phi_0)$ where ϕ_0 is the volume averaged porosity field. The rate of change of surface energy (80) is of order 10^{-2} at its largest and positive thus detracting from the net heat output; the net surface energy (α) thus obviously increases to a final value of $\phi_0^a(1 - \phi_0)^b$, since the surface area increases as this extreme damage reverses the effect of self-separation and the phases remix.

Finally, it is noteworthy that the measurable energy partitioning appears to be significantly different from the imposed deformational-work partitioning f . First, while the imposed partitioning f nominally controls the amount of deformational work applied to the creation of surface energy, the rate of change of this surface energy is in the end extremely small (whether positive or

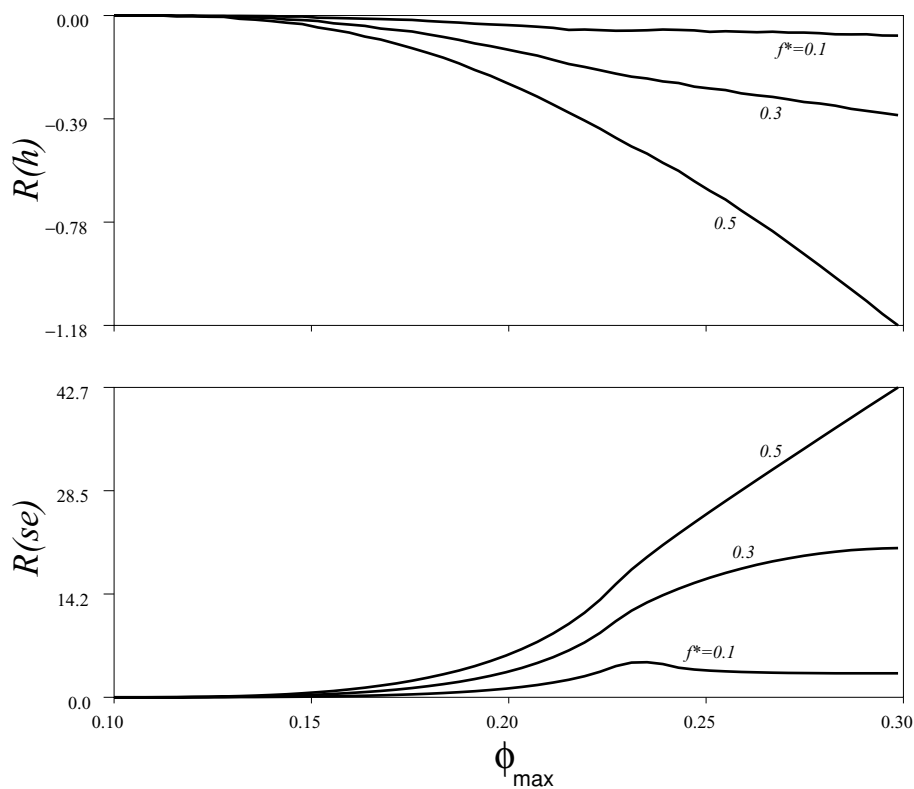


Figure 6. Relative heating and surface energy of cases in Fig. 5 with $f^* > 0$ to that with $f^* = 0$, versus peak porosity ϕ_{\max} . The quantities shown are percent relative heating $R(h) = (\langle \dot{\nu} \rangle_{f^*} - \langle \dot{\nu} \rangle_0) / \langle \dot{\nu} \rangle_0 \times 100$ and percent relative surface energy $R(se) = ((\alpha)_{f^*} - (\alpha)_0) / (\alpha)_0 \times 100$ (where subscript 0 implies the value at $f^* = 0$). These curves show that, relative to the undamaged system ($f^* = 0$), cases with finite damage ($f^* > 0$) generate less heat and more surface energy at a given peak porosity.

negative) relative to the imposed deformational work shown in the cases here. (An extremely small imposed shear stress Ω would perhaps cause a different result, but would require an even smaller γ which would then preclude any sharp-localization, as well as possibly much of the distributed damage solutions.) The rate of change in surface-energy is kept small by the internal dissipation term proportional to K which effectively dissipates the release of surface-energy back into heating. Second, while the influence of actual surface energy creation appears small, the largest effect on the net heat output appears to be in how the localizing porosity field changes the applied shear work $\Omega^2 \langle (1 - \phi)^{-1} \rangle$. In particular, cases with larger f^* localize faster but generate a porosity field that leads to a smaller net shear work than cases with smaller f^* and comparable peak porosity ϕ_{\max} (e.g. see Figs 5d and 6). This suggests that the measured energy partitioning is due more to the structure of the localized porosity field than to the amount of energy being stored as surface energy. In particular, one can compare the maximum net heating for curves in Fig. 5(d) corresponding to no damage $f^* = 0$, with heating of 2264, and maximum damage $f^* = 0.5$, with heating of approximately 2235; the measurable partitioning of energy apparent from this reduction in heating is very small, of order 0.01 (Fig. 6). Not only is this measured partitioning much smaller than nominally expected (given $f^* = 0.5$) but it is also not at all due to surface energy storage, which has only a negligible effect on the net heating. This measurable or apparent partitioning is instead almost entirely caused by the different values of $\Omega^2 \langle (1 - \phi)^{-1} \rangle$ for different f^* . Thus, the structure of the localization in ϕ creates an apparent energy partitioning that has little to do with the amount of energy stored on the interface.

9 DISCUSSION

9.1 Earth-like parameters

The primary dimensionless parameters controlling localization and energy exchange are the maximum partitioning fraction f^* , partitioning variability γ , and the fraction of shear deformational work going toward creation of surface energy $\nu = f^* \Omega^2 / \gamma$, where Ω is dimensionless effective shear rate. Neither f^* nor γ are easily estimated, although experiments imply that $f^* > O(10^{-1})$ is typical (Chrysochoos & Martin 1989; Chrysochoos *et al.* 1989, 1996), and our analysis above implies that strong localization is most pronounced for $\gamma \sim O(10^3)$ (see Fig. 2c), which requires $\Omega^2 \sim O(10^4 - 10^5)$, or $\Omega \sim O(10^2)$. We can thus estimate the dimensional shear stress $\sigma \alpha_0 \Omega$ (see eq. 60) required to cause a strong localization and thus plate-boundary formation in the lithosphere. The parameter α_0 is typically the inverse of grain size (Bercovici *et al.* 2001a; Ricard *et al.* 2001), and grain size varies widely from on the order of 1 cm to 1 μm , thus leading to the range $10^2 \text{ m}^{-1} \leq \alpha_0 \leq 10^6 \text{ m}^{-1}$. The surface energy σ of rocks is typically of order 1 J m^{-2} , although the effective fracture surface energy can be as high as 1000 J m^{-2} (Jaeger & Cook 1979; Cooper & Kohlstedt 1982; Atkinson 1987; Atkinson & Meredith 1987); however, we assume that this effective energy is due to an unmeasurable, perhaps fractal, property of fracture surface roughness and really represents extremely fine grain sizes. Thus we assume that the range in effective σ is actually due to the range in α_0 , and we therefore use either the full range in α_0 or σ , but not both; here we choose to set $\sigma = 1 \text{ J m}^{-2}$ and use the range of values of α_0 . In this case, the estimated shear stress to cause a

localization is in the range of $10^4 \text{ Pa} \leq \sigma\alpha_0\Omega \leq 10^8 \text{ Pa}$, or between 0.1 bar and 1 kbar, which is well within or less than the typical range of tectonic stresses; therefore, the stress conditions for strong localization via our proposed mechanism are readily available on Earth. Other Earth-like dimensional scales, such as the timescale for formation of localizations, are easily estimated using (60) and have been discussed already in Bercovici *et al.* (2001b).

9.2 The cost of making plates

Although the theory and calculations shown here are still rather idealized, they are motivated by the problem of generating plate tectonics, and more specifically plate boundaries on Earth (see reviews by Bercovici *et al.* 2000; Tackley 2000). Thus, as we are concerned here with the energy budget of localization, it is appropriate to discuss the energy costs of making plate boundaries.

The cause for how plate boundaries localize and evolve across the entire thickness of lithosphere is still not known. However, it is likely that the damage process (cracking and microcracking) is an important controlling mechanism. This is inferred because of the extreme weakening that can occur with such mechanisms and that is necessary to cause narrow boundaries (Bercovici 1998) possibly facilitated by liquid water (which is probably unique to Earth amongst the terrestrial planets); the prevalence of the microcracking brittle–ductile regime across the lithosphere (Kohlstedt *et al.* 1995; Evans & Kohlstedt 1995); and the tendency for reactivation of old faults which thus require long-lived weak zones (Gurnis *et al.* 2000). Thus, in considering general energy partitioning in shear-localization by damage, we can also estimate the energetics of making plate boundaries through similar processes.

To get an idea of the energy scales necessary to make a plate boundary, we can perform a rough calculation. Following our two-phase damage theory, the energy to create a narrow, damaged and thus high-porosity zone depends on the total amount of surface energy created. The amount of surface energy E_s per unit length ℓ along the damaged zone is

$$E_s/\ell = \sigma\alpha_0\phi^a(1 - \phi)^b D\delta \quad (81)$$

where D is the depth and δ the effective width of the damaged region. We assume the depth to be comparable to the depth of the brittle–ductile zone, roughly 10 km (Kohlstedt *et al.* 1995), while we assume the width to be effectively about 1 m thick, typical of the sum of all gouge zones in a plate boundary region (Mora & Place 1998); a thicker boundary region is certainly plausible, however, to be conservative we assume that if all the damaged region were confined to a uniform zone of reasonably high porosity, it would be of order 1 m. One can also argue that with fully developed faults, most deformation concentrates on the gouge region which is in essence the manifestation of an extreme localization. The range of values for the quantity $\sigma\alpha_0$ is as discussed above in the previous section. Finally, we assume the localized high-porosity region has $\phi \approx 0.1$. This leads to $3 \times 10^5 \text{ J m}^{-1} \leq E_s/\ell \leq 3 \times 10^9 \text{ J m}^{-1}$. A localized zone 1000 km long would require between $3 \times 10^{11} \text{ J}$ and $3 \times 10^{15} \text{ J}$ of energy.

However, perhaps a more meaningful quantity is the energy production rate which we can estimate from the velocity at which a localized zone effectively propagates. New plate boundaries are generally formed quite quickly relative to other geological processes. As an upper bound we can consider a rupture velocity V_r , which

is of the order of shear-wave velocity, i.e. $V_r \approx 3000 \text{ m s}^{-1}$ in the crust (chosen to be conservative). This leads to an energy production rate $E_s V_r/\ell$ between 10^9 W and 10^{13} W of energy. Although this is clearly an upper bound, it gives an approximate scale for the energy production rate. Considering the entire energy source for mantle convection is of the order of the Earth's net heat flux, i.e. $4 \times 10^{13} \text{ W}$, it is clear that the energy to make one localized plate boundary can range from being trivial (much less than the Earth's net heat flux) to extremely high (comparable to the net heat flux). Obviously, given the crudeness of this calculation, the Earth sits within this range since it has probably made many more than one plate boundary at a time.

If the energy necessary to make a plate boundary is at the high end of the range calculated, then this argues for the tendency to reactivate plate boundaries (Gurnis *et al.* 2000) since to do otherwise would be too costly in terms of available energy. It is also possible that the requisite energy to make the boundary is not readily withdrawn from the Earth's entire gravitational energy release, (e.g. the creation energy is too large and/or it only draws from the potential energy release of one plate, not the entire earth) and thus must be accumulated through elastic storage. Moreover, one could also surmise that since surface energy σ decreases with temperature, the efficacy of plate boundary generation in the presumably hotter Archaean would be greater, although the healing and annealing processes would probably be faster also. If the energy to make plate boundaries is at the low end of the range determined above, then plate generation should be facile at any time, under any condition, and on any planet, and reactivation less necessary, which is probably not the case.

Of course, an obvious question is that if the creation of plate boundary costs some net surface energy, relative to not making one, then why should it occur at all. However, the shear-localization calculations shown here demonstrate that it costs less net energy to force localization than to not force localization. In particular, although more surface energy is required (or in the calculations shown here less is released) to drive extreme localization, the extreme localizations result in less dissipative heating and thus in less net work required of the external forcing mechanism (Fig. 5). The concentration of a weak zone into a near singularity may cause extreme strain rates, but also confines dissipation to an extremely narrow region that in the end makes less contribution to the net dissipation and energy requirements.

This essential result was also demonstrated by Bercovici (1995) as an explanation for the cause of toroidal motion in a convecting mantle. The result is also similar to that found in granular-flow simulations which found that narrow gouge zones (well lubricated by rolling grains) are necessary to explain the anomalously low heat-flows along the San Andreas Fault system, otherwise known as the heat-flow paradox (Mora & Place 1998).

Our analysis, however, is most applicable for the formation of strike-slip boundaries and is not immediately applicable to the formation of other plate boundaries. In particular, mid-ocean ridges and subduction zones have the additional energy constraints of driving vertical mantle motion (which pure strike-slip zones do not). For example, while the formation of the weak zone necessary to initiate and maintain subduction is possibly analogous to our energy estimate above, this does not account for the work involved with bending a cold strong plate. Moreover, the localization of deformation at ridges is likely dominated by melting and focussing of melt percolation, both of which entail significantly different mechanisms than the one proposed here.

10 CONCLUSION

The work presented here in fact has three essential conclusions, which we summarize below:

10.1 Surface-energy partitioning

As shown in Bercovici *et al.* (2001a) and here, in order to pose a two-phase theory with interfacial energy, it is necessary to homogenize the phases and interface into an effective mixture such that the phases and interface and their properties exist at every point in some concentration. Although surface energy actually exists only on the interface, in the mixture approach it is effectively or mathematically distributed across the domain, and thus assumed to be distributed or partitioned between the phases. In Bercovici *et al.* (2001a) we assumed the surface energy is equipartitioned between phases. However, here we show that this approach leads to some minor inconsistencies (see Section 4.1) and that it is more plausible that the surface energy is effectively partitioned according to the phases' activation energy, parametrized by the phase viscosity. With this assumption, we are able to completely recover, in the limit of $\mu_m \gg \mu_f$, the melt-dynamics theory of McKenzie (1984) as well as the void theory of Ricard & Bercovici (submitted).

10.2 Localization and work-partitioning variability

Using this slightly adjusted theory, we examine cases of 1-D shear. As before (Bercovici *et al.* 2001b) we find that the growth rates of a localization are largely determined by the parameter $\nu = f^* \Omega^2 / \gamma$, where f^* is the maximum partitioning of deformational work toward creating surface energy, Ω is imposed shear stress and γ controls the variability of deformational-work partitioning (the larger γ the more slowly varying is the partitioning f). However, we also find that large values of γ are very important for generating sharp and nearly singular localizations. Although an increased γ requires a larger shear stress Ω to cause the same rate of localization (i.e. same ν), it will also suppress the tendency for dilation to dissipate nearly singular localization.

As found in Bercovici *et al.* (2001b), cases with very large ν (depending on the initial or background porosity) can lead to distributed damage and inhibition of localization of any kind (even stopping surface-tension driven self-separation). However, this regime also requires γ that are not too small, otherwise the range of solutions for this fragile state becomes vanishingly small.

10.3 Energy exchange between damage and heating

Finally, we examine the result on the energy and heat budget of the system for different maximum work partitioning rates f^* . After accounting for how the rate at which the system evolves depends on f^* , it is evident that the damage process causes the work input to be shunted toward surface energy production as expected; in the case of localization it slows down the release of surface energy, while with distributed damage it generates more interfacial surface energy. However, the more intense (i.e. narrow and faster growing) a localization the less net work is required to deform the system at a given stage of development (e.g. peak porosity), and thus less net heat is generated in the process. Thus while damage-driven localization causes more surface energy to be generated (relative to the situation with no damage), it also leads to a system with less net dissipation, less energy requirements, and thus overall greater efficiency.

ACKNOWLEDGMENTS

This work benefited greatly from discussions with Dan McKenzie. The authors also thank Harro Schmeling and two anonymous reviewers for their thoughtful comments. Support was provided by NSF (grant EAR-0105269), and the Centre National de la Recherche Scientifique (CNRS).

REFERENCES

- Atkinson, B., 1987. Introduction to fracture mechanics and its geophysical applications, in *Fracture Mechanics of Rock*, pp. 1–26, ed. Atkinson, B., Academic, San Diego, CA.
- Atkinson, B. & Meredith, P., 1987. Experimental fracture mechanics data for rocks and minerals, in *Fracture Mechanics of Rock*, pp. 427–525, ed. Atkinson, B., Academic, San Diego, CA.
- Bailyn, M., 1994. *A Survey of Thermodynamics*, Am. Inst. Phys., College Park, MD.
- Bender, C. & Orszag, S., 1978. *Advanced Mathematical Methods for Scientists and Engineers*, McGraw-Hill, Inc., New York.
- Bercovici, D., 1995. On the purpose of toroidal flow in a convecting mantle, *Geophys. Res. Lett.*, **22**, 3107–3110.
- Bercovici, D., 1998. Generation of plate tectonics from lithosphere-mantle flow and void-volatile self-lubrication, *Earth planet. Sci. Lett.*, **154**, 139–151.
- Bercovici, D., Ricard, Y. & Richards, M., 2000. The relation between mantle dynamics and plate tectonics: A primer, in *History and Dynamics of Global Plate Motions*, *Geophys. Monogr. Ser.*, Vol. 121, pp. 5–46, eds Richards, M.A., Gordon, R. & van der Hilst, R., AGU, Washington, DC.
- Bercovici, D., Ricard, Y. & Schubert, G., 2001a. A two-phase model of compaction and damage, 1. general theory, *J. geophys. Res.*, **106**, 8887–8906.
- Bercovici, D., Ricard, Y. & Schubert, G., 2001b. A two-phase model of compaction and damage, 3. applications to shear localization and plate boundary formation, *J. geophys. Res.*, **106**, 8925–8940.
- Bird, R., Stewart, W.E. & Lightfoot, E.N., 1960. *Transport Phenomena*, John Wiley, New York.
- Chrysochoos, A. & Martin, G., 1989. Tensile test microcalorimetry for thermomechanical behaviour law analysis, *Mater. Sci. Eng., A.*, **108**, 25–32.
- Chrysochoos, A., Maisonneuve, O., Martin, G., Caumon, H. & Chezeaux, J., 1989. Plastic and dissipated work and stored energy, *Nucl. Eng. Design*, **114**, 323–333.
- Chrysochoos, A., Pham, H. & Maisonneuve, O., 1996. Energy balance of thermoelastic martensite transformation under stress, *Nucl. Eng. Design*, **162**, 1–12.
- Cooper, R. & Kohlstedt, D., 1982. Interfacial energies in the olivine-basalt system, in *High Pressure Research in Geophysics*, *Adv. Earth Planet Sci.*, Vol. 12, pp. 217–228, eds Akimoto, S. & Manghnani, M., Cent. For Acad. Pub., Tokyo.
- Desjournères, M. & Spanjaard, D., 1993. *Concepts in Surface Physics*, Springer-Verlag, New York.
- Drew, D. & Segel, L., 1971. Averaged equations for two-phase flows, *Stud. Appl. Math.*, **50**, 205–257.
- Evans, B. & Kohlstedt, D., 1995. Rheology of rocks, in *Rock Physics and Phase Relations: A Handbook of Physical Constants*, *AGU Ref. Shelf*, Vol. 3, pp. 148–165, ed. Ahrens, T.J., AGU, Washington, DC.
- Farren, W. & Taylor, G., 1925. The heat developed during plastic extension of metals, *Proc. R. Soc. Lond., A*, **107**, 422–451.
- Guéguen, Y. & Palciauskas, V., 1994. *Introduction to the Physics of Rocks*, Princeton Univ. Press, New Jersey.
- Gurnis, M., Zhong, S. & Toth, J., 2000. On the competing roles of fault reactivation and brittle failure in generating plate tectonics from mantle convection, in *History and Dynamics of Global Plate Motions*, *Geophys. Monogr. Ser.*, Vol. 121, pp. 73–94, eds Richards, M., Gordon, R. & van der Hilst, R., AGU, Washington, DC.
- Hansen, N. & Schreyer, H., 1992. Thermodynamically consistent theories for elastoplasticity coupled with damage, in *Damage Mechanics and*

- Localization*, pp. 53–67, eds Ju, J. & Valanis, K., Am. Soc. of Mech. Eng., New York.
- Jaeger, J. & Cook, N., 1979. *Fundamentals of Rock Mechanics*, 3rd edn, Chapman and Hall, New York.
- Kohlstedt, D., Evans, B. & Mackwell, S., 1995. Strength of the lithosphere: Constraints imposed by laboratory experiments, *J. geophys. Res.*, **100**, 17 587–17 602.
- Lemaitre, J., 1992. *A Course on Damage Mechanics*, Springer-Verlag, New York.
- Lemonds, J. & Needleman, A., 1986. Finite element analyses of shear localization in rate and temperature dependent solids, *Mech. Mater.*, **5**, 339–361.
- Lyakhovskiy, V., Ben-Zion, Y. & Agnon, A., 1997. Distributed damage, faulting, and friction, *J. geophys. Res.*, **102**, 27 635–27 649.
- Mathur, K., Needleman, A. & Tvergaard, V., 1996. Three dimensional analysis of dynamic ductile crack growth in a thin plate, *J. Mech. Phys. Solids*, **44**, 439–464.
- McKenzie, D., 1984. The generation and compaction of partially molten rock, *J. Petrol.*, **25**, 713–765.
- McKenzie, D., 1985. The extraction of magma from the crust and mantle, *Earth planet. Sci. Lett.*, **74**, 81–91.
- McKenzie, D., 1987. The compaction of igneous and sedimentary rocks, *J. geol. Soc. Lond.*, **144**, 299–307.
- McKenzie, D. & Holness, M., 2000. Local deformation in compacting flows: Development of pressure shadows, *Earth planet. Sci. Lett.*, **180**, 169–184.
- Mora, P. & Place, D., 1998. Numerical simulation of earthquake faults with gouge; toward a comprehensive explanation for the heat flow paradox, *J. geophys. Res.*, **103**, 21 067–21 089.
- Ni, J. & Beckerman, C., 1991. A volume-averaged two-phase model for transport phenomena during solidification, *Metall. Trans. B*, **22**, 349–361.
- Povirk, G., Nutt, S. & Needleman, A., 1994. Continuum modelling of residual stresses in metal-matrix composites, in *Residual Stress in Composites*, pp. 3–23, eds Barrera, B. & Dutta, V., TMS, New York.
- Prutton, M., 1983. *Surface Physics*, Oxford University Press, New York.
- Regenauer-Lieb, K., 1999. Dilatant plasticity applied to alpine collision: Ductile void-growth in the intraplate area beneath the eifel volcanic field, *J. Geodyn.*, **27**, 1–21.
- Ricard, Y. & Bercovici, D., 2003. Two-phase damage theory and crustal rock failure: the theoretical “void” limit, and the prediction of experimental data, *Geophys. J. Int.*, submitted to.
- Ricard, Y., Bercovici, D. & Schubert, G., 2001. A two-phase model of compaction and damage, 2, applications to compaction, deformation, and the role of interfacial surface tension, *J. geophys. Res.*, **106**, 8907–8924.
- Schmeling, H., 2000. Partial melting and melt segregation in a convecting mantle, in *Physics and Chemistry of Partially Molten Rocks*, pp. 141–178, eds Bagdassarov, N., Laporte, D. & Thompson, A., Kluwer Academic, Norwell, Mass.
- Spiegelman, M., 1993a. Flow in deformable porous media, part 1, simple analysis, *J. Fluid Mech.*, **247**, 17–38.
- Spiegelman, M., 1993b. Flow in deformable porous media, part 2, numerical analysis—the relationship between shock waves and solitary waves, *J. Fluid Mech.*, **247**, 39–63.
- Spiegelman, M., 1993. Physics of melt extraction: Theory, implications and applications, *Phil. Trans. R. Soc. Lond., A*, **342**, 23–41.
- Sumita, I., Yoshida, S., Kumazawa, M. & Hamano, Y., 1996. A model for sedimentary compaction of a viscous medium and its application to inner-core growth, *Geophys. J. Int.*, **124**, 502–524.
- Tackley, P., 2000. The quest for self-consistent generation of plate tectonics in mantle convection models, in *History and Dynamics of Global Plate Motions*, *Geophys. Monogr. Ser.*, Vol. 121, pp. 47–72, eds Richards, M.A., Gordon, R. & van der Hilst, R., AGU, Washington, DC.
- Taylor, G. & Quinney, H., 1934. The latent energy remaining in metal after cold working, *Proc. R. Soc. Lond., A*, **143**, 307–326.
- Turcotte, D. & Schubert, G., 1982. *Geodynamics*, John Wiley & Sons, New York.